Journal of Sound and Vibration 327 (2009) 55–69

Contents lists available at ScienceDirect

Journal of Sound and Vibration

journal homepage: www.elsevier.com/locate/jsvi

Frequency response of bimodular cross-ply laminated cylindrical panels

K. Khan, B.P. Patel *, Y. Nath

Department of Applied Mechanics, Indian Institute of Technology Delhi, New Delhi 110016, India

ARTICLE INFO

Article history:
Received 14 February 2009
Received in revised form
9 May 2009
Accepted 21 May 2009
Handling Editor: C.L. Morfey
Available online 18 June 2009

ABSTRACT

With the in-plane inertia, the response of bimodular material laminated cylindrical panels computed using direct time integration shows numerical instability. This instability is due to the sudden change in the restoring force from positive/negative half cycle to negative/positive half cycle. The sudden change in restoring force with in-plane inertia excites higher harmonics at every instant of a cycle change leading to numerical instability. This numerical instability can be eliminated if the switch over from positive to negative half cycle or vice versa is exactly at the instant when restoring force is zero. However all the elements of restoring force vector do not become zero simultaneously when direct time integration is performed. Thus it is not possible in the numerical time integration approach to find time instant when restoring force vector becomes a null vector. Therefore, an approach based on Galerkin method in time domain is proposed for the steady-state response of bimodular material structures that eliminates the instability. Its efficacy is demonstrated for the first time for frequency response of bimodular material laminated cylindrical panels modelled using finite element based on Bert's constitutive model.

1. Introduction

The time domain numerical integration techniques are quite well established in the area of structural dynamics for unimodular materials. These techniques may predict the frequency response of bimodulus structures without considering in-plane inertia for a very limited range of cases. In the presence of in-plane inertia, the sudden change of restoring force from positive/negative half cycle to negative/positive half cycle excites higher harmonics at every instant of cycle change leading to numerical instability in the time marching scheme. It is not possible to eliminate this instability by switching over at the instant when restoring force vector is null since elements of displacement vector do not cross zero simultaneously in a numerical time integration. Thus these methods fail to predict the steady-state/frequency response of bimodular structures. This difficulty has been overcome by developing a methodology based on time domain Galerkin approach. This is not the sole purpose of the present study but also to give bench mark solutions for frequency response of bimodular cylindrical panels. It should be kept in mind that frequency response of bimodulus structures is not dealt in the open literature. Therefore, the present investigation may be attributed to an effort that addresses both the above aspects.

The literature on the dynamics of bimodulus structures, either free vibration or forced vibration analyses, is quite limited [1–7]. The free vibration analysis of bimodular material cross-ply laminated rectangular plates is carried out by Bert et al. [1], Doong and Chen [2], Doong and Fung [3]. Patel et al. [4] have carried out the free vibration analysis of angle-ply

* Corresponding author. Tel.: +91 11 26591232; fax: +91 11 26581119.
E-mail address: badripatel@hotmail.com (B.P. Patel).

0022-460X/$ - see front matter © 2009 Elsevier Ltd. All rights reserved.
doi:10.1016/j.jsv.2009.05.026

laminated bimodulus thick rectangular plates. The free vibration analysis of cross-ply and angle-ply cylindrical panels is carried out by Bert and Kumar [5] and Khan et al. [6,7], respectively. The free vibration of cross-ply conical panels is carried out by Khan et al. [8]. The transient response of bimodular rectangular plates is studied by Reddy [9] and Patel et al. [10] wherein the investigation/analysis is limited to first cycle only.

The steady-state frequency response of bimodulus laminated structures has not received the attention of researchers in the open literature. The frequency response is important for the design of such structures under dynamic loading.

Adopting the fiber direction strain governed constitutive model due to Bert [11], the steady-state response of bimodulus material laminated cylindrical panels is studied using finite element method based on first-order shear deformation theory. The solution of governing equations is obtained using two approaches: (i) direct time integration (Newmark's constant–average acceleration scheme) till steady state is reached for different forcing frequencies and (ii) Galerkin approach wherein the steady-state solution is assumed in the form of a Fourier series. Some of the results obtained from both the approaches are compared. It is found that for bimodulus laminates with significant difference in the positive and negative half cycle frequencies, the direct time integration approach fails to predict steady-state response. The influence of geometrical parameters, lamination scheme and boundary conditions on steady-state response of bimodulus material laminated cylindrical panels is investigated.

2. Formulation

The geometry and coordinate system of a cylindrical panel with total thickness h, radius r, meridional length L, circumferential length b and sector angle Ψ is shown in Fig. 1. The displacement field (u, v, w) at a point (s, θ, z) is expressed as function of middle surface displacements u_0, v_0, w_0 and independent rotations β_s and β_θ of the meridional and hoop sections, respectively, as

$$u(s,\theta,z,t) = u_0(s,\theta,t) + z\beta_s(s,\theta,t)$$

$$v(s,\theta,z,t) = v_0(s,\theta,t) + z\beta_\theta(s,\theta,t)$$

$$w(s,\theta,z,t) = w_0(s,\theta,t) \tag{1}$$

The analysis is carried out using finite element formulation based on Bert's constitutive model [1] and Sanders [12] type kinematic approximations. The finite element used is a C^0 eight-noded serendipity quadrilateral shear flexible shell element with 5 degrees of freedom (u_0, v_0, w_0, β_s, β_θ) developed based on the field consistency approach [13]. The details of the finite element formulation and its validation for free vibration analysis of bimodular material laminated plates/shells can be found in Ref. [7].

The governing equations of motion, considering dissipative forces, take the form

$$[\mathbf{M}]\{\ddot{\boldsymbol{\delta}}\} + [\mathbf{C}]\{\dot{\boldsymbol{\delta}}\} + [\mathbf{K}]\{\boldsymbol{\delta}\} = \{\mathbf{F}\} \tag{2}$$

where [**M**], [**K**] and [**C**] are global mass, stiffness and damping matrices, and {**F**} is consistent global load vector. The damping matrix is taken proportional to mass matrix as: $[\mathbf{C}] = \beta[\mathbf{M}]$; $\beta = 2\xi\omega$, where ξ is modal damping factor and ω is

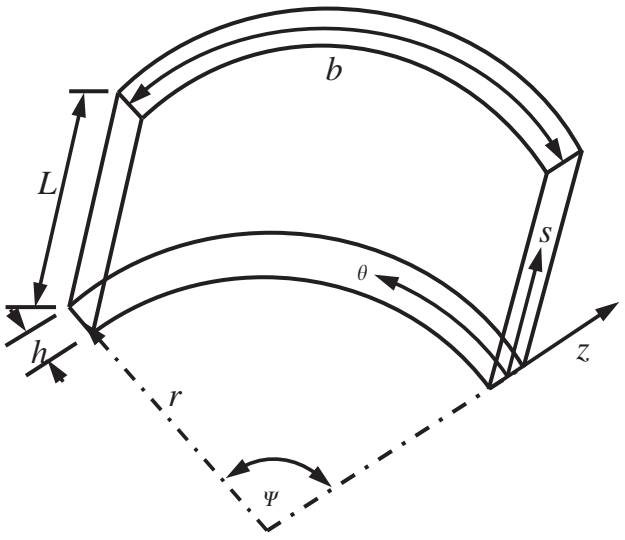

Fig. 1. Geometry and coordinate system of cylindrical panel.

natural frequency. Assuming solution $\{\boldsymbol{\delta}\} = \{\bar{\boldsymbol{\delta}}\}e^{i\omega t}$ for undamped free vibration, Eq. (2) becomes

$$[\mathbf{K}]\{\bar{\boldsymbol{\delta}}\} = \omega^2[\mathbf{M}]\{\bar{\boldsymbol{\delta}}\} \tag{3}$$

Free vibration frequencies and corresponding modal vectors are extracted using iterative eigenvalue approach [7].

3. Solution method

For the forced response analysis, the solution of Eq. (2) is obtained using two approaches: (i) direct time integration (Newmark's constant–average acceleration) [14] till steady state is reached and (ii) Galerkin approach wherein the steady-state solution is assumed in the form of a Fourier series. Some of the results obtained from both the approaches are compared. It is found that for bimodulus laminates with significant difference in the positive and negative half cycle free vibration frequencies, the direct time integration approach fails to predict steady-state response.

The solution procedure based on Galerkin's approach is discussed here.

3.1. Galerkin approach

The steady-state forced response of panels subjected to uniformly distributed harmonic excitation ($q = q_0 \operatorname{Cos}\omega_F t$) is obtained using Galerkin method in time domain. The solution is assumed as

$$\{\boldsymbol{\delta}\} = \{\boldsymbol{\delta_0}\} + \sum_{i=1}^{m}(\{\boldsymbol{\delta_{ci}}\}\operatorname{Cos} i\omega_F t + \{\boldsymbol{\delta_{si}}\}\operatorname{Sin} i\omega_F t) \tag{4}$$

where ω_F is forcing frequency and t is time.

Substituting Eq. (4) in Eq. (2), the residual vector $\{\mathbf{R}\}$ is written as

$$\begin{aligned}\{\mathbf{R}\} = &-\omega_F^2[\mathbf{M}]\sum_{i=1}^{m} i^2(\{\boldsymbol{\delta_{ci}}\}\operatorname{Cos} i\omega_F t + \{\boldsymbol{\delta_{si}}\}\operatorname{Sin} i\omega_F t) - \omega_F[\mathbf{C}]\sum_{i=1}^{m} i(\{\boldsymbol{\delta_{ci}}\}\operatorname{Sin} i\omega_F t - \{\boldsymbol{\delta_{si}}\}\operatorname{Cos} i\omega_F t)\\ &+ [\mathbf{K}]\{\boldsymbol{\delta_0}\} + [\mathbf{K}]\sum_{i=1}^{m}(\{\boldsymbol{\delta_{ci}}\}\operatorname{Cos} i\omega_F t + \{\boldsymbol{\delta_{si}}\}\operatorname{Sin} i\omega_F t) - \{\mathbf{F}\}\end{aligned} \tag{5}$$

To generate the $(2m+1)n$ equations in terms of $(2m+1)n$ unknowns ($\{\boldsymbol{\delta_0}\}, \{\boldsymbol{\delta_{ci}}\}, \{\boldsymbol{\delta_{si}}\}$, $i = 1,2,\ldots,m$), the weighted integral of residual $\{\mathbf{R}\}$ over one time period is equated to zero for weighting functions: 1, $\operatorname{Cos} i\omega_F t$, $\operatorname{Sin} i\omega_F t$, $i = 1,2,\ldots,m$. For each weighting function (say $\operatorname{Cos} i\omega_F t$), the integration w.r.t time is performed piecewise as follows:

$$\int_0^{t_1}\{\mathbf{R}\}\operatorname{Cos} i\omega_F t\,dt + \int_{t_1}^{t_2}\{\mathbf{R}\}\operatorname{Cos} i\omega_F t\,dt + \int_{t_2}^{2\pi/\omega_F}\{\mathbf{R}\}\operatorname{Cos} i\omega_F t\,dt = 0 \tag{6}$$

Here t_1 and t_2 are time instants within a cycle when response changes from positive/negative half cycle to negative/positive half cycle (see Fig. 2). It may be noted that $\{\mathbf{R}\}$ is different for positive and negative half cycles since the stiffness matrix $[\mathbf{K}]$ is different for positive (say $[\mathbf{K_1}]$) and negative (say $[\mathbf{K_2}]$) half cycles.

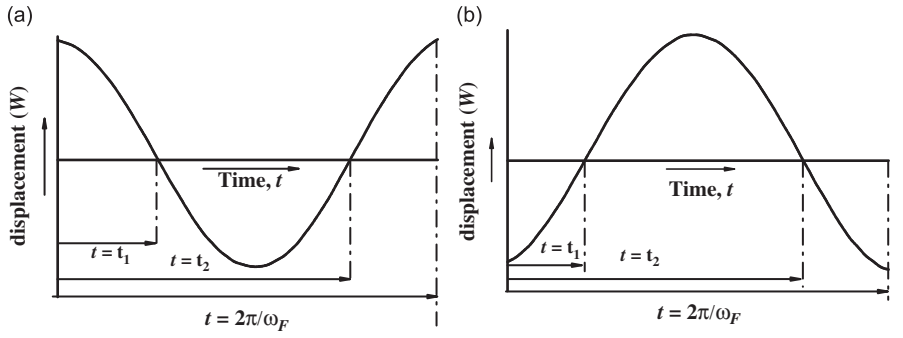

Fig. 2. Response during two portions of a vibration cycle of bimodular panel.

The final set of equations, considering all the $(2m+1)$ weighting functions, is written as

$$\begin{bmatrix} [\mathbf{A_{0,0}}] & [\mathbf{A_{0,c1}}] & [\mathbf{A_{0,s1}}] & \cdot & [\mathbf{A_{0,cj}}] & [\mathbf{A_{0,sj}}] & \cdot & \cdot & \cdot & \cdot & \cdot \\ [\mathbf{A_{c1,0}}] & [\mathbf{A_{c1,c1}}] & [\mathbf{A_{c1,s1}}] & \cdot & [\mathbf{A_{c1,cj}}] & [\mathbf{A_{c1,sj}}] & \cdot & \cdot & \cdot & \cdot & \cdot \\ [\mathbf{A_{s1,0}}] & [\mathbf{A_{s1,c1}}] & [\mathbf{A_{s1,s1}}] & \cdot & [\mathbf{A_{s1,cj}}] & [\mathbf{A_{s1,sj}}] & \cdot & \cdot & \cdot & \cdot & \cdot \\ \cdot & \cdot & \cdot & \cdot & \cdot & \cdot & \cdot & \cdot & \cdot & \cdot & \cdot \\ \cdot & \cdot & \cdot & \cdot & \cdot & \cdot & \cdot & \cdot & \cdot & \cdot & \cdot \\ \cdot & \cdot & \cdot & \cdot & \cdot & \cdot & \cdot & \cdot & \cdot & \cdot & \cdot \\ \cdot & \cdot & \cdot & \cdot & \cdot & \cdot & \cdot & \cdot & \cdot & \cdot & \cdot \\ [\mathbf{A_{ci,0}}] & [\mathbf{A_{ci,c1}}] & [\mathbf{A_{ci,s1}}] & \cdot & [\mathbf{A_{ci,cj}}] & [\mathbf{A_{ci,sj}}] & \cdot & \cdot & \cdot & \cdot & \cdot \\ [\mathbf{A_{si,0}}] & [\mathbf{A_{si,c1}}] & [\mathbf{A_{si,s1}}] & \cdot & [\mathbf{A_{si,cj}}] & [\mathbf{A_{si,sj}}] & \cdot & \cdot & \cdot & \cdot & \cdot \\ \cdot & \cdot & \cdot & \cdot & \cdot & \cdot & \cdot & \cdot & \cdot & \cdot & \cdot \\ \cdot & \cdot & \cdot & \cdot & \cdot & \cdot & \cdot & \cdot & \cdot & \cdot & \cdot \end{bmatrix} \begin{Bmatrix} \{\boldsymbol{\delta_0}\} \\ \{\boldsymbol{\delta_{c1}}\} \\ \{\boldsymbol{\delta_{s1}}\} \\ \cdot \\ \{\boldsymbol{\delta_{cj}}\} \\ \{\boldsymbol{\delta_{sj}}\} \\ \cdot \\ \cdot \\ \cdot \\ \cdot \end{Bmatrix} = \begin{Bmatrix} \{\mathbf{0}\} \\ (\pi/\omega_F)\{\mathbf{F_0}\} \\ \{\mathbf{0}\} \\ \cdot \\ \{\mathbf{0}\} \\ \{\mathbf{0}\} \\ \cdot \\ \{\mathbf{0}\} \\ \{\mathbf{0}\} \\ \cdot \\ \cdot \end{Bmatrix} \tag{7}$$

where coefficient sub-matrices of Eq. (7), for motion from 0 to t_1 and t_2 to $2\pi/\omega_F$ corresponding to positive half cycle and that from t_1 to t_2 corresponding to negative half cycle, are expressed as

$$[\mathbf{A_{0,0}}] = [\mathbf{K_1}](t_1 - t_2 + 2\pi/\omega_F) + [\mathbf{K_2}](t_2 - t_1);$$

$$[\mathbf{A_{0,cj}}] = [[\mathbf{K_1}] - [\mathbf{K_2}]](\mathrm{Sin\,j}\omega_F t_1 - \mathrm{Sin\,j}\omega_F t_2)/(\mathrm{j}\omega_F), \quad j = 1, \ldots, m;$$

$$[\mathbf{A_{0,sj}}] = [[\mathbf{K_1}] - [\mathbf{K_2}]](\mathrm{Cos\,j}\omega_F t_2 - \mathrm{Cos\,j}\omega_F t_1)/(\mathrm{j}\omega_F), \quad j = 1, \ldots, m;$$

$$[\mathbf{A_{ci,0}}] = [[\mathbf{K_1}] - [\mathbf{K_2}]](\mathrm{Sin\,i}\omega_F t_1 - \mathrm{Sin\,i}\omega_F t_2)/(\mathrm{i}\omega_F), \quad i = 1, \ldots, m;$$

$$[\mathbf{A_{si,0}}] = [[\mathbf{K_1}] - [\mathbf{K_2}]](\mathrm{Cos\,i}\omega_F t_2 - \mathrm{Cos\,i}\omega_F t_1)/(\mathrm{i}\omega_F), \quad i = 1, \ldots, m;$$

For $i \neq j$:

$$[\mathbf{A_{ci,cj}}] = [[\mathbf{K_1}] - [\mathbf{K_2}]]((\mathrm{Sin}(i+j)\omega_F t_1 - \mathrm{Sin}(i+j)\omega_F t_2)/(i+j) + (\mathrm{Sin}(i-j)\omega_F t_1 - \mathrm{Sin}(i-j)\omega_F t_2)/(i-j))/(2\omega_F);$$

$$[\mathbf{A_{ci,sj}}] = [[\mathbf{K_1}] - [\mathbf{K_2}]]((\mathrm{Cos}(i+j)\omega_F t_1 - \mathrm{Cos}(i+j)\omega_F t_2)/(i+j) + (\mathrm{Cos}(i-j)\omega_F t_1 - \mathrm{Cos}(i-j)\omega_F t_2)/(i-j))/(2\omega_F);$$

$$[\mathbf{A_{si,cj}}] = [[\mathbf{K_1}] - [\mathbf{K_2}]]((\mathrm{Cos}(i+j)\omega_F t_2 - \mathrm{Cos}(i+j)\omega_F t_1)/(i+j) + (\mathrm{Cos}(i-j)\omega_F t_2 - \mathrm{Cos}(i-j)\omega_F t_1)/(i-j))/(2\omega_F);$$

$$[\mathbf{A_{si,sj}}] = [[\mathbf{K_1}] - [\mathbf{K_2}]]((\mathrm{Sin}(i+j)\omega_F t_2 - \mathrm{Sin}(i+j)\omega_F t_1)/(i+j) + (\mathrm{Sin}(i-j)\omega_F t_1 - \mathrm{Sin}(i-j)\omega_F t_2)/(i-j))/(2\omega_F);$$

For $i = j$:

$$[\mathbf{A_{ci,cj}}] = [[\mathbf{K_1}] - [\mathbf{K_2}]]((t1 - t2)/2 + (\mathrm{Sin\,2i}\omega_F t_1 - \mathrm{Sin\,2i}\omega_F t_2)/(4\mathrm{i}\omega_F)) + [\mathbf{K_1}](\pi/\omega_F) - [\mathbf{M}]\pi \mathrm{i}^2 \omega_F;$$

$$[\mathbf{A_{ci,sj}}] = [[\mathbf{K_1}] - [\mathbf{K_2}]](\mathrm{Cos\,2i}\omega_F t_2 - \mathrm{Cos\,2i}\omega_F t_1)/(4\mathrm{i}\omega_F) + [\mathbf{C}]\mathrm{i}\pi;$$

$$[\mathbf{A_{si,cj}}] = [[\mathbf{K_1}] - [\mathbf{K_2}]](\mathrm{Cos\,2i}\omega_F t_2 - \mathrm{Cos\,2i}\omega_F t_1)/(4\mathrm{i}\omega_F) - [\mathbf{C}]\mathrm{i}\pi;$$

$$[\mathbf{A_{si,sj}}] = [[\mathbf{K_1}] - [\mathbf{K_2}]]((t1 - t2)/2 - (\mathrm{Sin\,2i}\omega_F t_1 - \mathrm{Sin\,2i}\omega_F t_2)/(4\mathrm{i}\omega_F)) + [\mathbf{K_1}](\pi/\omega_F) - [\mathbf{M}]\pi \mathrm{i}^2 \omega_F.$$

In the above expressions, $[\mathbf{K_1}]$ and $[\mathbf{K_2}]$ are interchanged if motion from 0 to t_1 and t_2 to $2\pi/\omega_F$ corresponds to negative half cycle and that from t_1 to t_2 corresponds to positive half cycle.

Since t_1 and t_2 are not known *a priori*, two additional equations are required. These equations are obtained by equating the transverse displacement at an anti-node point of a mode (frequency response is studied here in the neighbourhood of a free vibration frequency) to zero at t_1 and t_2 as follows:

$$w_{00} + \sum_{i=1}^{m} (w_{0ci}\,\mathrm{Cos\,i}\omega_F t_1 + w_{0si}\,\mathrm{Sin\,i}\omega_F t_1) = 0 \tag{8}$$

$$w_{00} + \sum_{i=1}^{m} (w_{0ci}\,\mathrm{Cos\,i}\omega_F t_2 + w_{0si}\,\mathrm{Sin\,i}\omega_F t_2) = 0 \tag{9}$$

Eqs. (7)–(9) constitute $(2m+1)n+2$ nonlinear (due to unknowns t_1 and t_2) equations in $(2m+1)n+2$ unknowns. In order to obtain the solution of these equations using Newton–Raphson iterative technique, the incremental equations can be

written as

$$\begin{bmatrix} [\mathbf{A_{0,0}}] & [\mathbf{A_{0,c1}}] & [\mathbf{A_{0,s1}}] & . & [\mathbf{A_{0,cj}}] & [\mathbf{A_{0,sj}}] & . & . & . & . & . \\ [\mathbf{A_{c1,0}}] & [\mathbf{A_{c1,c1}}] & [\mathbf{A_{c1,s1}}] & . & [\mathbf{A_{c1,cj}}] & [\mathbf{A_{c1,sj}}] & . & . & . & . & . \\ [\mathbf{A_{s1,0}}] & [\mathbf{A_{s1,c1}}] & [\mathbf{A_{s1,s1}}] & . & [\mathbf{A_{s1,cj}}] & [\mathbf{A_{s1,sj}}] & . & . & . & . & . \\ . & . & . & . & . & . & . & . & . & . & . \\ . & . & . & . & . & . & . & . & . & . & . \\ . & . & . & . & . & . & . & . & . & . & . \\ . & . & . & . & . & . & . & . & . & . & . \\ [\mathbf{A_{ci,0}}] & [\mathbf{A_{ci,c1}}] & [\mathbf{A_{ci,s1}}] & . & [\mathbf{A_{ci,cj}}] & [\mathbf{A_{ci,sj}}] & . & . & . & . & . \\ [\mathbf{A_{si,0}}] & [\mathbf{A_{si,c1}}] & [\mathbf{A_{si,s1}}] & . & [\mathbf{A_{si,cj}}] & [\mathbf{A_{si,sj}}] & . & . & . & . & . \\ . & . & . & . & . & . & . & . & . & . & . \\ . & . & . & . & . & . & . & . & . & . & . \end{bmatrix} \begin{Bmatrix} \{\Delta\boldsymbol{\delta}_\mathbf{0}\} \\ \{\Delta\boldsymbol{\delta}_\mathbf{c1}\} \\ \{\Delta\boldsymbol{\delta}_\mathbf{s1}\} \\ . \\ \{\Delta\boldsymbol{\delta}_\mathbf{cj}\} \\ \{\Delta\boldsymbol{\delta}_\mathbf{sj}\} \\ . \\ . \\ . \\ . \end{Bmatrix} = \begin{Bmatrix} \{\mathbf{r_0}\} \\ \{\mathbf{r_{c1}}\} \\ \{\mathbf{r_{s1}}\} \\ . \\ . \\ . \\ . \\ \{\mathbf{r_{ci}}\} \\ \{\mathbf{r_{si}}\} \\ . \\ . \end{Bmatrix} \tag{10}$$

where

$$\{\mathbf{r_0}\} = -[\mathbf{A_{0,0}}]\{\boldsymbol{\delta}_\mathbf{0}\} - \sum_{j=1}^{m}([\mathbf{A_{0,cj}}]\{\boldsymbol{\delta}_\mathbf{cj}\} + [\mathbf{A_{0,sj}}]\{\boldsymbol{\delta}_\mathbf{sj}\}) - \{\mathbf{f_{0,1}}\}\Delta t_1 - \{\mathbf{f_{0,2}}\}\Delta t_2;$$

$$\{\mathbf{r_{c1}}\} = (\pi/\omega_F)\{\mathbf{F_0}\} - [\mathbf{A_{c1,0}}]\{\boldsymbol{\delta}_\mathbf{0}\} - \sum_{j=1}^{m}([\mathbf{A_{c1,cj}}]\{\boldsymbol{\delta}_\mathbf{cj}\} + [\mathbf{A_{c1,sj}}]\{\boldsymbol{\delta}_\mathbf{sj}\}) - \{\mathbf{f_{c1,1}}\}\Delta t_1 - \{\mathbf{f_{c1,2}}\}\Delta t_2;$$

$$\{\mathbf{r_{s1}}\} = -[\mathbf{A_{s1,0}}]\{\boldsymbol{\delta}_\mathbf{0}\} - \sum_{j=1}^{m}([\mathbf{A_{s1,cj}}]\{\boldsymbol{\delta}_\mathbf{cj}\} + [\mathbf{A_{s1,sj}}]\{\boldsymbol{\delta}_\mathbf{sj}\}) - \{\mathbf{f_{s1,1}}\}\Delta t_1 - \{\mathbf{f_{s1,2}}\}\Delta t_2;$$

$$\{\mathbf{r_{ci}}\} = -[\mathbf{A_{ci,0}}]\{\boldsymbol{\delta}_\mathbf{0}\} - \sum_{j=1}^{m}([\mathbf{A_{ci,cj}}]\{\boldsymbol{\delta}_\mathbf{cj}\} + [\mathbf{A_{ci,sj}}]\{\boldsymbol{\delta}_\mathbf{sj}\}) - \{\mathbf{f_{ci,1}}\}\Delta t_1 - \{\mathbf{f_{ci,2}}\}\Delta t_2, \quad i = 2,3,4,\ldots,m;$$

$$\{\mathbf{r_{si}}\} = -[\mathbf{A_{si,0}}]\{\boldsymbol{\delta}_\mathbf{0}\} - \sum_{j=1}^{m}([\mathbf{A_{si,cj}}]\{\boldsymbol{\delta}_\mathbf{cj}\} + [\mathbf{A_{si,sj}}]\{\boldsymbol{\delta}_\mathbf{sj}\}) - \{\mathbf{f_{si,1}}\}\Delta t_1 - \{\mathbf{f_{si,2}}\}\Delta t_2;$$

$$\{\mathbf{f_{0,p}}\} = \left[\frac{\partial \mathbf{A_{0,0}}}{\partial \mathbf{t_p}}\right]\{\boldsymbol{\delta}_\mathbf{0}\} + \sum_{j=1}^{m}\left(\left[\frac{\partial \mathbf{A_{0,cj}}}{\partial \mathbf{t_p}}\right]\{\boldsymbol{\delta}_\mathbf{cj}\} + \left[\frac{\partial \mathbf{A_{0,sj}}}{\partial \mathbf{t_p}}\right]\{\boldsymbol{\delta}_\mathbf{sj}\}\right), \quad p = 1,2;$$

$$\{\mathbf{f_{ci,p}}\} = \left[\frac{\partial \mathbf{A_{ci,0}}}{\partial \mathbf{t_p}}\right]\{\boldsymbol{\delta}_\mathbf{0}\} + \sum_{j=1}^{m}\left(\left[\frac{\partial \mathbf{A_{ci,cj}}}{\partial \mathbf{t_p}}\right]\{\boldsymbol{\delta}_\mathbf{cj}\} + \left[\frac{\partial \mathbf{A_{ci,sj}}}{\partial \mathbf{t_p}}\right]\{\boldsymbol{\delta}_\mathbf{sj}\}\right), \quad i = 1,2,3,\ldots,m;$$

$$\{\mathbf{f_{si,p}}\} = \left[\frac{\partial \mathbf{A_{si,0}}}{\partial \mathbf{t_p}}\right]\{\boldsymbol{\delta}_\mathbf{0}\} + \sum_{j=1}^{m}\left(\left[\frac{\partial \mathbf{A_{si,cj}}}{\partial \mathbf{t_p}}\right]\{\boldsymbol{\delta}_\mathbf{cj}\} + \left[\frac{\partial \mathbf{A_{si,sj}}}{\partial \mathbf{t_p}}\right]\{\boldsymbol{\delta}_\mathbf{sj}\}\right).$$

The coefficient matrix of Eq. (10) is unsymmetric and sparse but the nonzero coefficients are scattered throughout. It may be noted that the matrices in Eq. (2) are symmetric and banded with semi-bandwidth (n_b) being much smaller than the total number of unknowns (n). Eq. (10) is rearranged so that the rearranged equations are banded with semi-bandwidth equal to m times n_b.

The incremental forms of Eqs. (8) and (9) are written as

$$\Delta w_{00} + \sum_{i=1}^{m}(\Delta w_{0ci}\,\mathrm{Cos}\,\mathrm{i}\omega_F t_1 + \Delta w_{0si}\,\mathrm{Sin}\,\mathrm{i}\omega_F t_1) + \left(\sum_{i=1}^{m}(-w_{0ci}\mathrm{Sin}\,\mathrm{i}\omega_F t_1 + w_{0si}\,\mathrm{Cos}\,\mathrm{i}\omega_F t_1)\mathrm{i}\omega_F\right)\Delta t_1 = 0 \tag{11a}$$

$$\Delta w_{00} + \sum_{i=1}^{m}(\Delta w_{0ci}\,\mathrm{Cos}\,\mathrm{i}\omega_F t_2 + \Delta w_{0si}\,\mathrm{Sin}\,\mathrm{i}\omega_F t_2) + \left(\sum_{i=1}^{m}(-w_{0ci}\mathrm{Sin}\,\mathrm{i}\omega_F t_2 + w_{0si}\,\mathrm{Cos}\,\mathrm{i}\omega_F t_2)\mathrm{i}\omega_F\right)\Delta t_2 = 0 \tag{11b}$$

First, Eq. (10) is used to express the incremental displacement vectors ($\{\boldsymbol{\Delta\delta}_\mathbf{0}\}, \{\boldsymbol{\Delta\delta}_\mathbf{ci}\}, \{\boldsymbol{\Delta\delta}_\mathbf{si}\}$, $i = 1, 2, 3,\ldots,m$) in terms of Δt_1 and Δt_2. This solution is substituted in Eq. (11) and the resulting equations are solved for Δt_1 and Δt_2, and in turn, incremental displacement vectors are obtained. To start the solution, forcing frequency ratio (ω_F/ω, ω is fundamental free vibration frequency) is taken as 0.9. At this starting point, displacement vectors are initialized to zero, and t_1 and t_2 are assumed as $\pi/(2\omega_F)$ and $3\pi/(2\omega_F)$, respectively. With these starting values, the iteration is continued till the solution

converges to the specified convergence tolerance (each incremental displacement becomes less than 10^{-7}). Then the forcing frequency is incremented. With the solution of the previous step as starting point, the converged solution for new forcing frequency is obtained. This is repeated till solution up to the desired forcing frequency is obtained.

When ω_F/ω crosses 1, the phase lag of response becomes greater than 90°. At forcing frequency ratio greater than one, t_1 becomes negative if iteration continued from previous solution. For this case, values of t_1 and t_2 are reinitialized at the starting iteration so that these lie in the range 0 to $2\pi/\omega_F$.

For the parameters considered in the present study, the detailed analysis revealed that the participation of higher harmonics is quite important but their participation is limited to the extent that the displacement of anti-node point crosses zero displacement only twice within an excitation period and hence the piecewise integration, as given in Eq. (6), is valid. If this displacement crosses more than twice, then the response period has to be divided accordingly for performing the integrations similar to Eq. (6) and correspondingly the number of unknowns corresponding to zero crossing time will increase. This can easily be incorporated in the developed Galerkin's based solution methodology presented.

4. Results and discussion

Based on the progressive mesh refinement, 10×10 mesh is found to be adequate to model the full panels. The material properties considered in the analysis are [6]:

In tension: $E_{1t} = 3.58\,\text{GPa}$, $E_{2t} = E_{3t} = 0.00909\,\text{GPa}$, $G_{12t} = G_{13t} = 0.0037\,\text{GPa}$, $G_{23t} = 0.0029\,\text{GPa}$, $v_{12t} = v_{23t} = v_{13t} = 0.416$.

In compression: $E_{1c} = E_{2c} = E_{3c} = 0.012\,\text{GPa}$, $G_{12c} = G_{13c} = 0.0037\,\text{GPa}$, $G_{23c} = 0.00499\,\text{GPa}$, $v_{12c} = v_{23c} = v_{13c} = 0.205$.

Density $\rho = 970\,\text{Kg/m}^3$ is same in tension and compression. The modal damping factor (ξ) is taken as 0.01 for the steady-state frequency response analysis.

Boundary conditions considered are:

Simply supported:	$u_0 = w_0 = \beta_s = 0$ $v_0 = w_0 = \beta_\theta = 0$	at $\theta = 0$ and b/r (straight edges) at $s = 0$ and L (curved edges)
Clamped:	$u_0 = v_0 = w_0 = \beta_s = \beta_\theta = 0$	at straight/curved edges

The various combinations of edge conditions considered are: straight edges simply supported and curved edges clamped (SCSC), all edges simply supported (SSSS), straight edges clamped and curved edges simply supported (CSCS). The transverse displacement is presented in the nondimensional form as: $W = w_0 h^3 E_{2c}/(q_0 L^4)$. The fundamental free vibration frequency $\omega = 2(1/\omega_1 + 1/\omega_2)^{-1}$, where ω_1 and ω_2 are free vibration frequencies corresponding positive and negative half cycles, respectively.

Since the results are not available for steady-state response of bimodulus material laminated structures, the present formulation is validated considering transient response. The results are presented in Fig. 3 for bimodular cross-ply

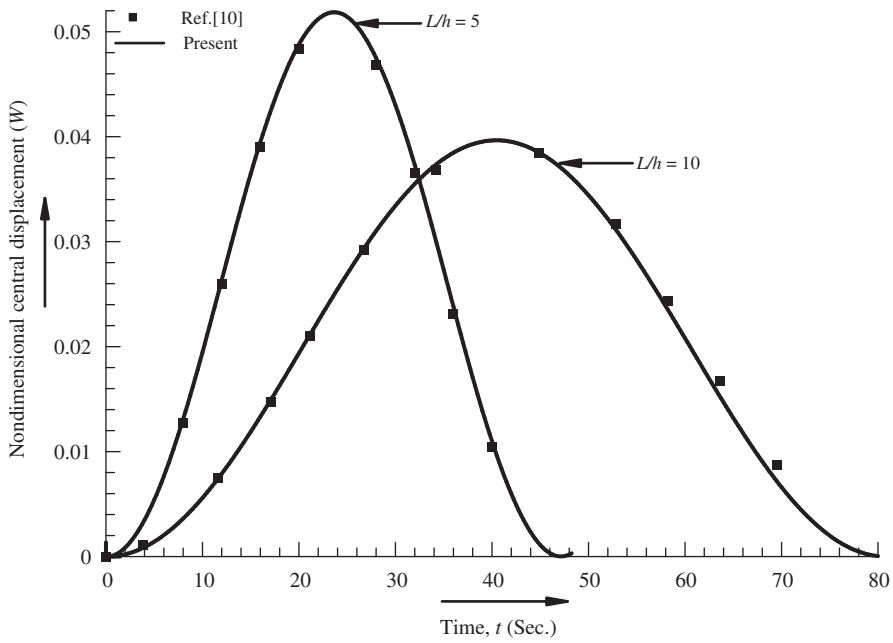

Fig. 3. Comparison of transverse displacement history of two-layered cross-ply (0°/90°) square bimodular laminate ($L/b = 1$).

laminated $(0^\circ/90^\circ)$ simply supported square plate. It can be seen from this figure that the present results are in good agreement with those of Ref. [10].

The response of eight-layered cross-ply $(0^\circ/90^\circ)_4$ bimodular SCSC panel ($L/b = 1$, $b/h = 10$, $r/h = 100$, $\xi = 0.01$) subjected to uniformly distributed harmonic excitation ($q = q_0 \operatorname{Cos} \omega_F t$) is obtained using Newmark direct time integration scheme ($\Delta t = \pi/100\omega_F$). The time versus nondimensional central transverse displacement response is shown in Fig. 4 with and without considering in-plane inertia. It can be seen from this figure that the steady state is reached when in-plane inertia is not considered. With the in-plane inertia, the response shows unstable nature after few cycles. This instability in the direct time integration approach is due to the sudden change in the restoring force ($[\mathbf{K}]\{\boldsymbol{\delta}\}$) when response changes from positive/

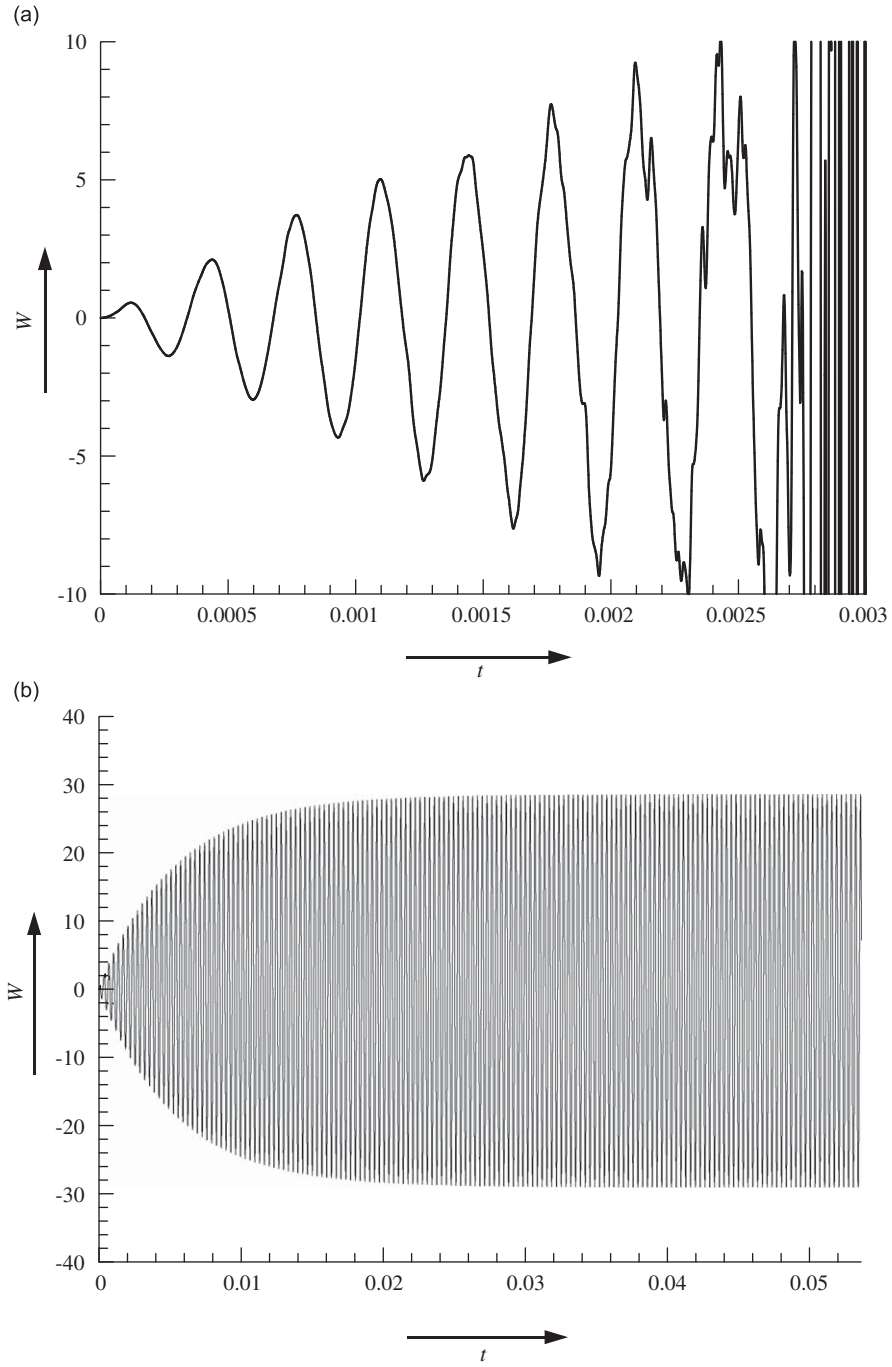

Fig. 4. Nondimensional transverse central displacement (W) history of eight-layered cross-ply $(0^\circ/90^\circ)_4$ bimodular SCSC panel ($L/b = 1$, $b/h = 10$, $r/h = 100$): (a) with in-plane inertia and (b) without in-plane inertia.

negative half cycle to negative/positive half cycle. The change in the restoring force components corresponding to in-plane displacements (u_0, v_0) is greater than those corresponding to transverse displacement (w). The abrupt change in restoring force with in-plane inertia excites higher harmonics at every instant of a cycle change leading to numerical instability. This numerical instability can be eliminated if the switch over from positive to negative half cycle or vice versa is exactly at the instant when restoring force becomes zero. The zero restoring force corresponds to the null displacement vector ($\{\boldsymbol{\delta}\} = \{\mathbf{0}\}$).

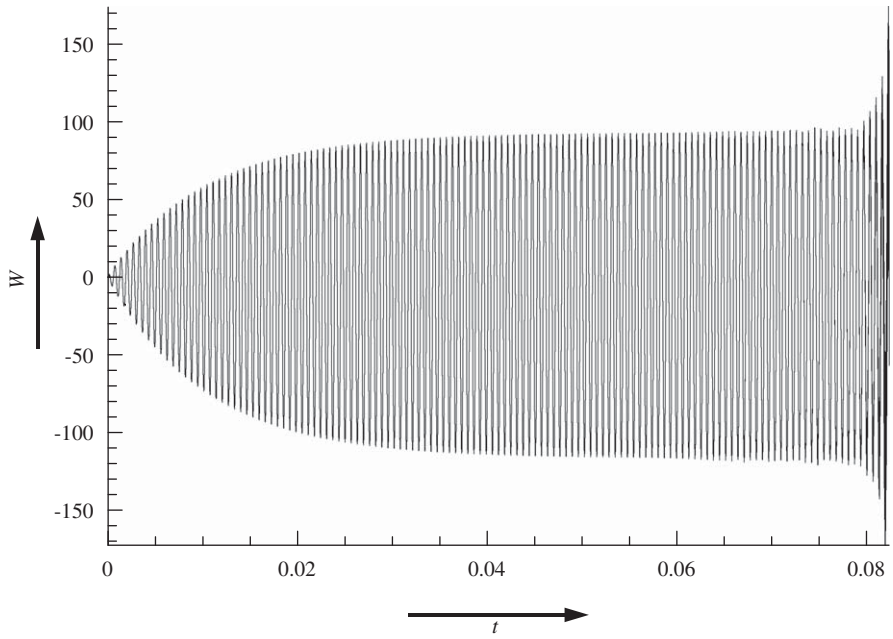

Fig. 5. Nondimensional transverse central displacement (W) history of eight-layered cross-ply $(0^\circ/90^\circ)_4$ bimodular SSSS panel ($L/b = 1$, $b/h = 10$, $r/h = 20$, $\omega_{Fl}\omega = 1.0$) without in-plane inertia ($\omega_1 = 29\,608.329$ rad/s, $\omega_2 = 10\,796.7197$ rad/s, $100(\omega_1 - \omega_2)/\omega_1 = 20.18$).

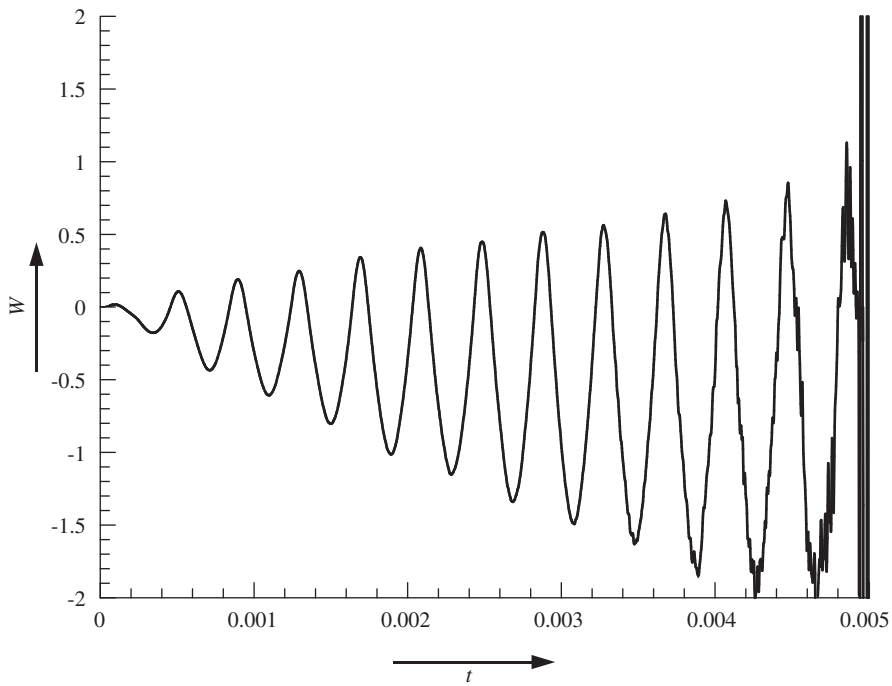

Fig. 6. Nondimensional transverse central displacement (W) history of two-layered cross-ply $(0^\circ/90^\circ)$ bimodular CSCS panel ($L/b = 2$, $b/h = 10$, $r/h = 50$, $\omega_{Fl}\omega = 1.0$) without in-plane inertia ($\omega_1 = 29608.329$ rad/s, $\omega_2 = 10796.7197$ rad/s, $100\ (\omega_1 - \omega_2)/\omega_1 = 64.27$).

However, it is found that the all the elements of displacement vector do not become zero simultaneously when direct time integration is performed. Thus it is not possible in the direct numerical time integration approach to find the time instant when restoring force vector goes to zero. In some cases (particularly in the direct numerical time integration approach

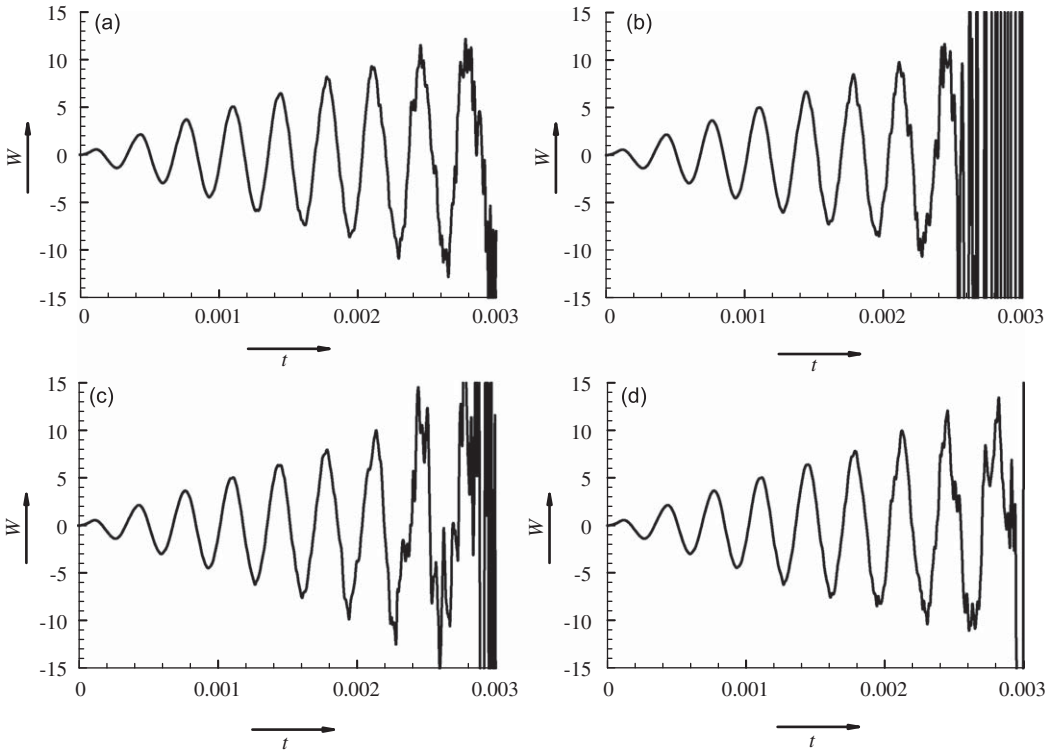

Fig. 7. Nondimensional transverse central displacement (W) history of eight-layered cross-ply $(0^\circ/90^\circ)_4$ bimodular SCSC panel ($L/b = 1$, $b/h = 10$, $r/h = 100$) with in-plane inertia: (a) $\Delta t = \pi/200\omega_F$, (b) $\Delta t = \pi/400\omega_F$, (c) $\Delta t = \pi/800\omega_F$ and (d) $\Delta t = \pi/3000\omega_F$).

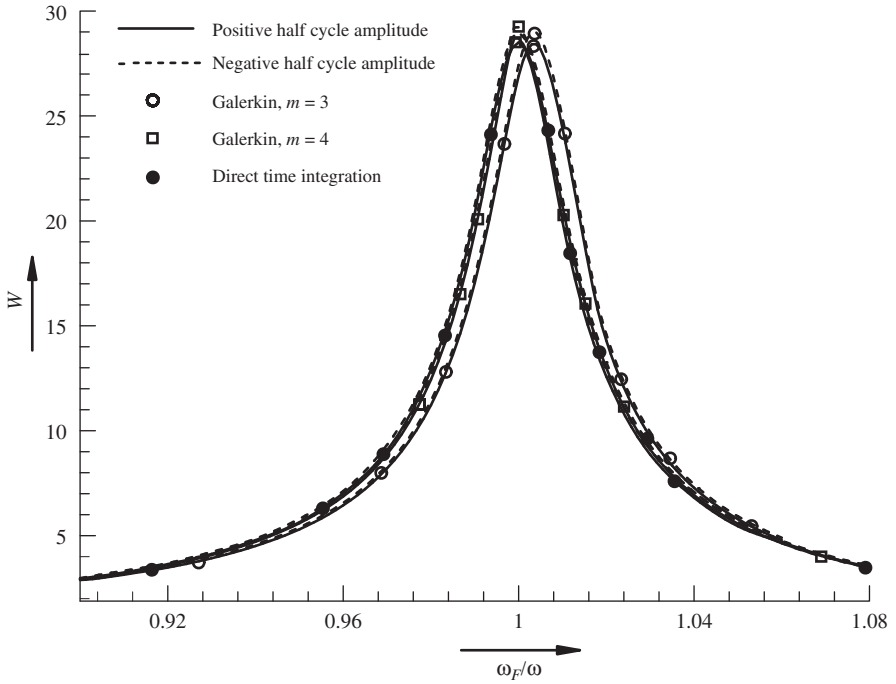

Fig. 8. Comparision of frequency response of eight-layered cross-ply $(0^\circ/90^\circ)_4$ SCSC panel ($L/b = 1$, $b/h = 10$, $r/h = 100$) without in-plane inertia.

when percentage difference of positive and negative half cycle free vibration frequencies is larger) even without in-plane inertia, the numerical instability occurs (Figs. 5 and 6). This is due to the sudden change in restoring force corresponding to transverse displacement. The time integration is also performed with smaller time steps ($\Delta t = \pi/200\omega_F$, $\pi/400\omega_F$, $\pi/800\omega_F$, $\pi/3000\omega_F$), however, the numerical instability continue to occur at slightly later time instants (Fig. 7). Therefore, the detailed results obtained using proposed Galerkin method based approach are presented.

The frequency response of eight-layered $(0^\circ/90^\circ)_4$ bimodular SCSC panel ($L/b = 1$, $r/h = 100$, $b/h = 10$) without considering in-plane inertia is studied. The results obtained using Galerkin and direct time integration approaches are shown in Fig. 8. It can be seen that the Galerkin solution with $m = 4$ matches very well with the direct time integration approach. The convergence study for eight-layered $(0^\circ/90^\circ)_4$ SSSS panel ($L/b = 1$, $r/h = 20$, $b/h = 10$) considering in-plane inertia is shown in Fig. 9. It can be seen from this figure that the solution with $m = 6$ is quite accurate. The convergence is established for both displacement amplitude as well as ω_F/ω ratio corresponding to peak displacement amplitude. It is interesting to note that with the increase in the number of terms (m), the occurrence of maximum central deflection approaches to $\omega_F/\omega = 1$. To demonstrate the efficacy of the Galerkin based approach, the results presented for different boundary conditions, geometrical and lamination parameters are discussed next.

The effects of aspect ratio (L/b), radius-to-thickness ratio (r/h) and number of layers (N) on the frequency response of cross-ply laminated SCSC panels ($b/h = 10$) are shown in Figs. 10 and 11. It can be seen from these results that with the increase in L/b, nondimensional amplitude (W) decreases and percentage difference of positive and negative half cycle amplitudes increases. The effect of r/h ratio on frequency response is not significant. As number of layers increases, the percentage difference of positive and negative half cycle amplitudes decreases. The participation of various harmonics (values of w_{00}, w_{0ci} and w_{0si}) in the forced response of two-layered $(0^\circ/90^\circ)$ SCSC panel ($L/b = 2$, $r/h = 50$, $b/h = 10$) is given in Table 1. The comparison of frequency response of unimodular (with tensile/compressive/average properties) and bimodular eight-layered $(0^\circ/90^\circ)_4$ SCSC panel ($L/b = 1$, $r/h = 100$, $b/h = 10$) is shown in Fig. 12. It can be seen from this figure that the bimodularity has significant effect on the frequency response.

The effect of b/h ratio on the frequency response of two- and eight-layered SCSC panels ($L/b = 1$, $r/h = 100$, $b/h = 20, 40, 50$) is shown in Fig. 13. It can be seen that the nondimensional transverse displacement amplitude decreases with the increase in b/h. The percentage difference of amplitudes of two- and eight-layered panels increases with the increase in b/h.

The frequency response of two-layered $(0^\circ/90^\circ)$ SSSS panel ($L/b = 0.5, 1.0$; $r/h = 20, 50, 100$; $b/h = 10$) is shown in Fig. 14. The response is qualitatively similar to SCSC panels. But, the percentage difference of positive and negative half cycle amplitudes is significant. The influence of r/h is more on positive half cycle amplitude for $L/b = 0.5$. The local distortions of the frequency response curves for some cases are due to the changes in the relative participation of higher harmonics.

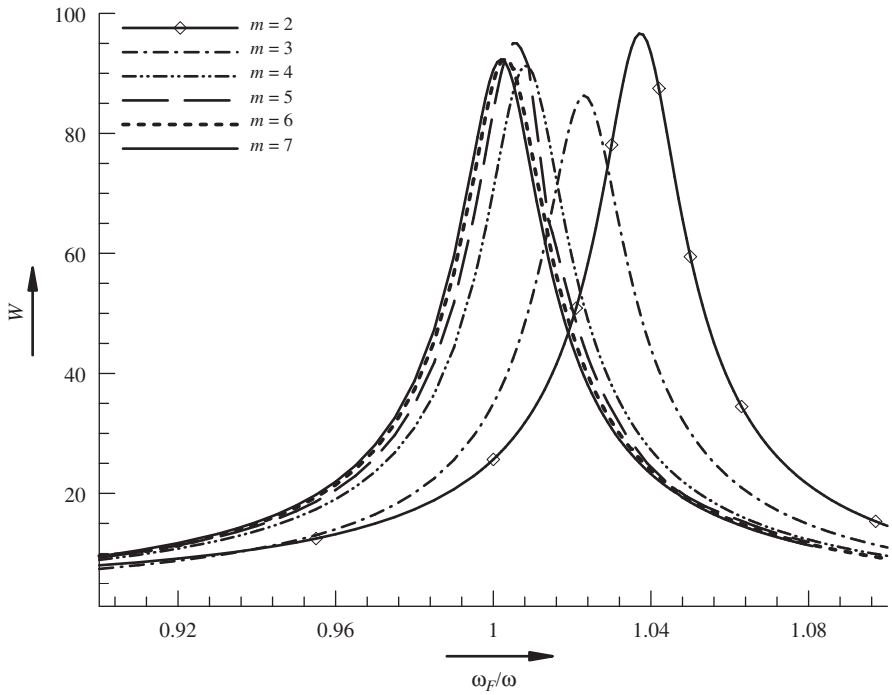

Fig. 9. Convergence study for frequency response of eight-layered cross-ply $(0^\circ/90^\circ)_4$ SSSS panel ($L/b = 1$, $b/h = 10$, $r/h = 20$) with in-plane inertia.

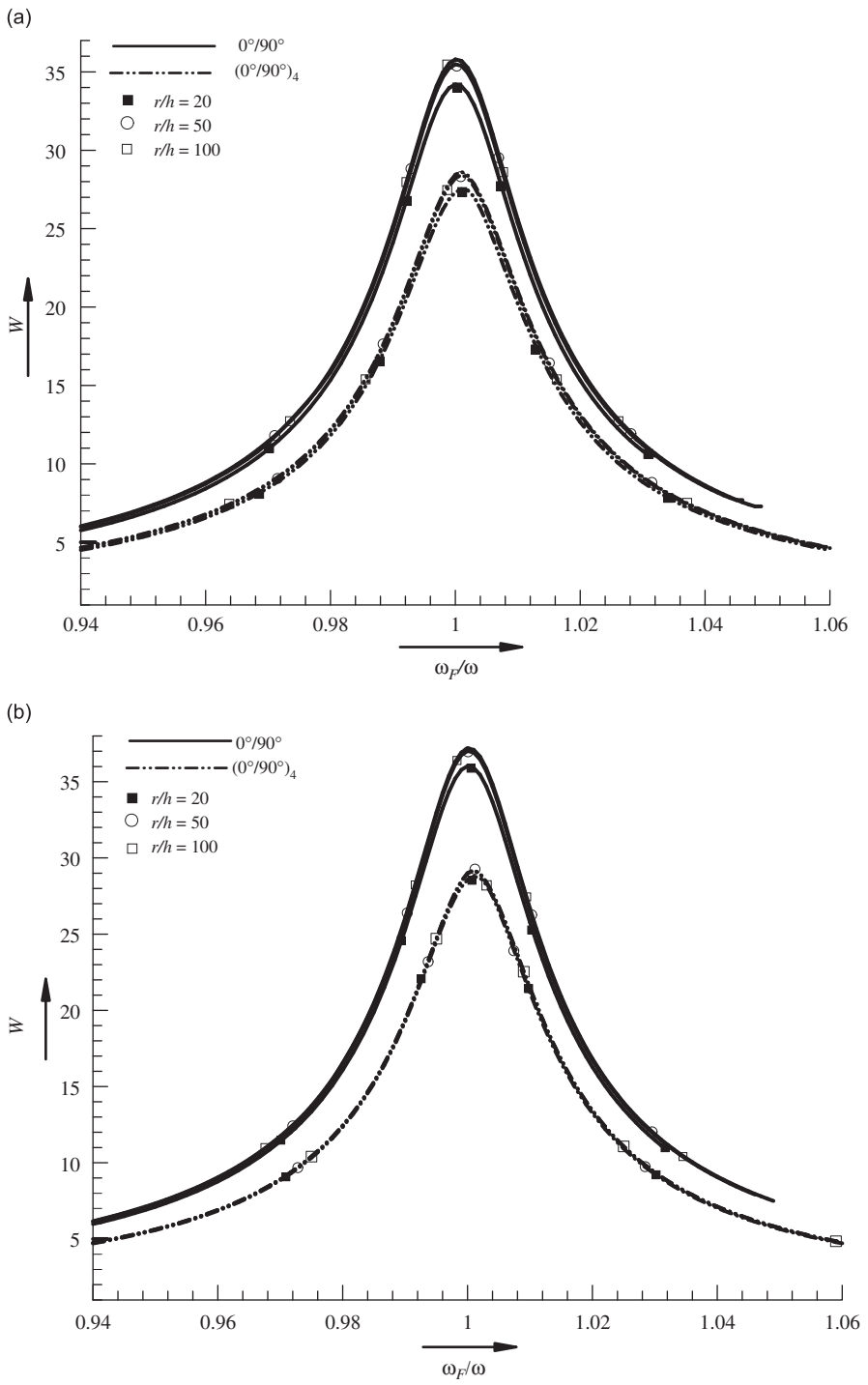

Fig. 10. Frequency response of two- and eight-layered cross-ply SCSC panel ($L/b = 1$, $b/h = 10$) with in-plane inertia: (a) positive half cycle amplitude and (b) negative half cycle amplitude.

5. Conclusion

The forced dynamic response of bimodulus material laminated cylindrical panels is studied using finite element method based on first-order shear deformation theory and Bert's constitutive model. The solution of governing equations is obtained using direct time integration and Galerkin approach. It is found that for bimodulus laminates with significant difference in the positive and negative half cycle frequencies, the direct time integration approach fails to predict

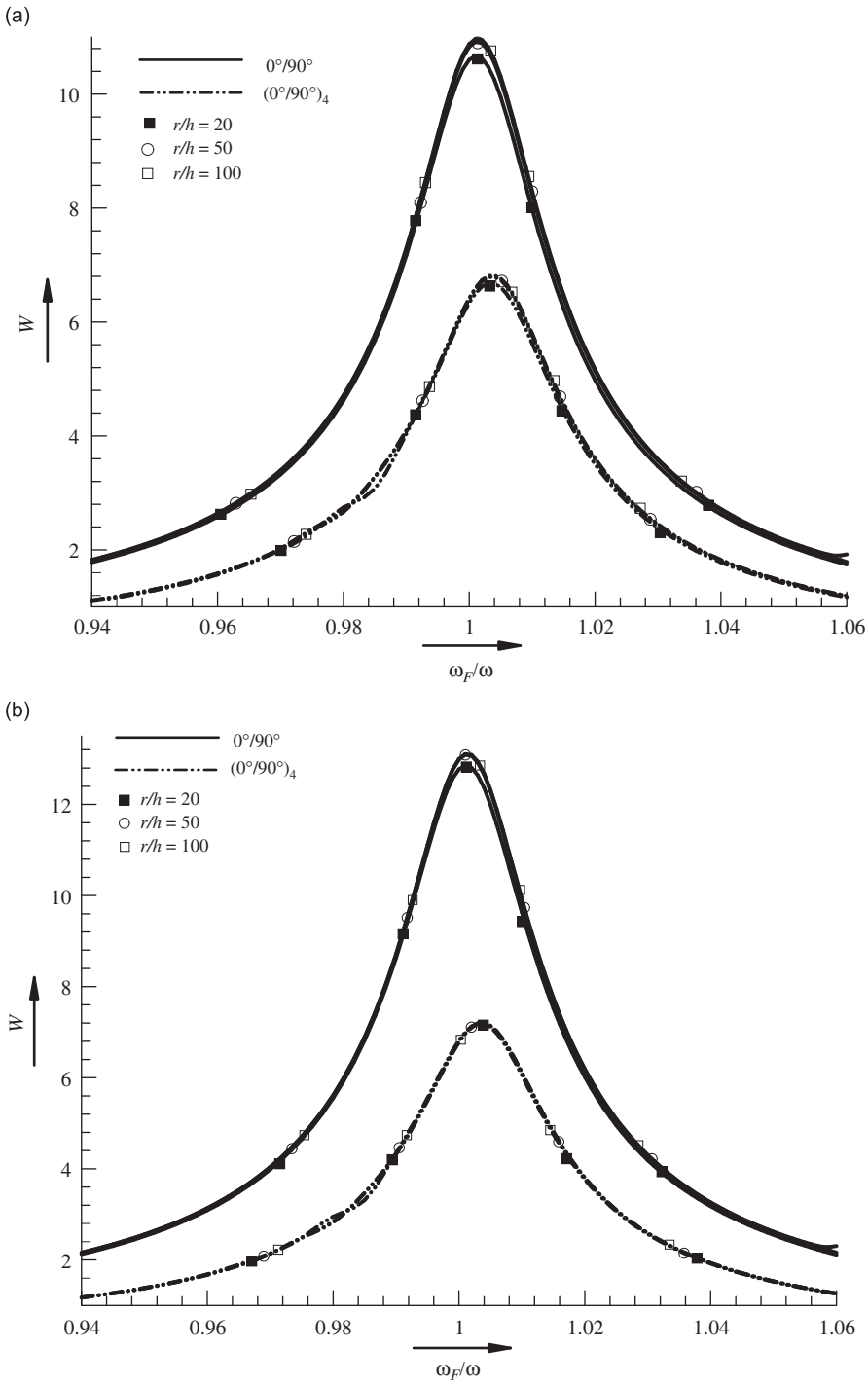

Fig. 11. Frequency response of two- and eight-layered cross-ply SCSC panel ($L/b = 2$, $b/h = 10$) with in-plane inertia: (a) positive half cycle amplitude and (b) negative half cycle amplitude.

Table 1
Participation of various harmonics in the forced response of two-layered ($0^\circ/90^\circ$) SCSC panel ($L/b = 2$, $r/h = 50$, $b/h = 10$).

ω_F/ω	w_0	w_{c1}	w_{s1}	w_{c2}	w_{s2}	w_{c3}	w_{s3}	w_{c4}	w_{s4}	w_{c5}	w_{s5}	w_{c6}	w_{s6}
0.995	−1.233	5.165	9.269	−0.136	0.217	−0.012	0.060	−0.0006	0.0089	0.0015	0.0034	−0.0239	−0.2703
1.0	−1.395	0.688	12.004	−0.271	0.037	−0.007	−0.011	-0.0062	0.00007	−0.0004	0.0043	−0.0998	0.0758
1.005	−1.273	−4.425	10.042	−0.173	−0.179	0.0107	−0.0014	0.0013	−0.0060	−0.0007	−0.0018	0.0404	−0.0388

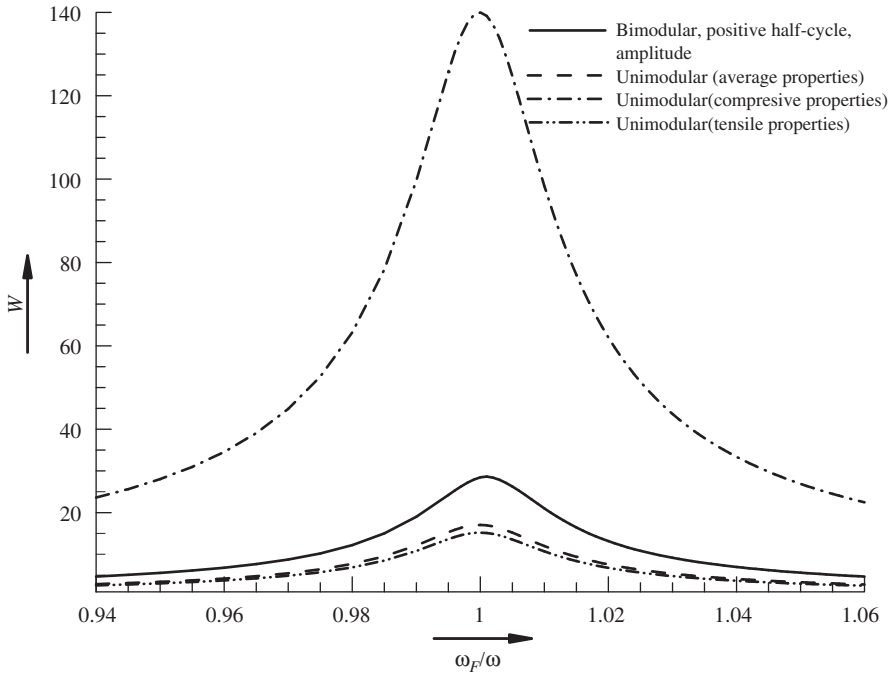

Fig. 12. Comparision of frequency response of unimodular and bimodular eight-layered cross-ply $(0^\circ/90^\circ)_4$ SCSC panel ($L/b = 1$, $b/h = 10$, $r/h = 100$) with in-plane inertia.

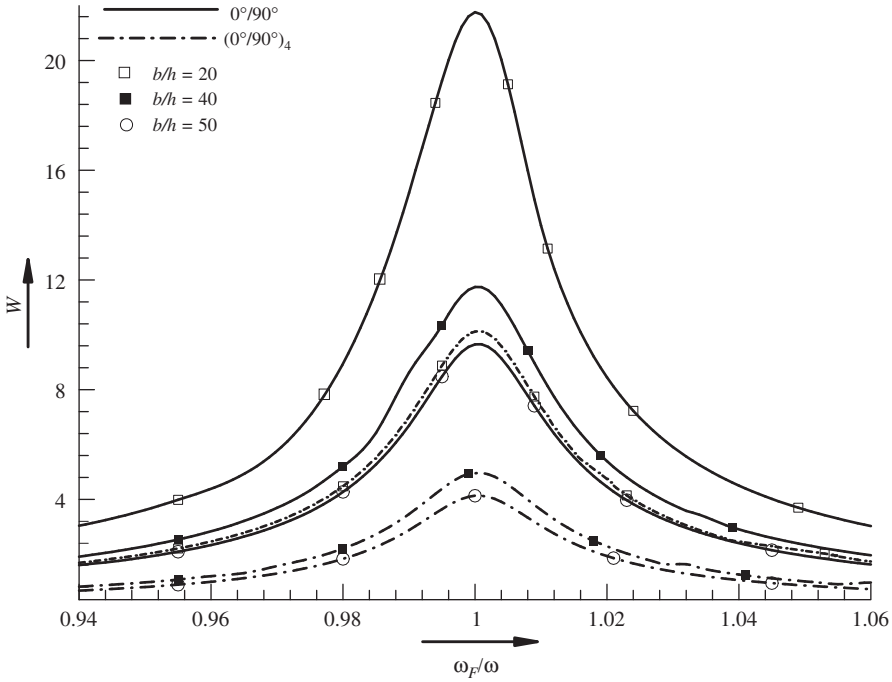

Fig. 13. Frequency response of two- and eight-layered cross-ply SCSC panel ($L/b = 1$, $r/h = 100$) with in-plane inertia for different b/h.

steady-state response due to numerical instability. This instability due to the sudden change in the restoring force can be eliminated if the switch over from positive to negative half cycle or vice versa is exactly at the instant when restoring force is zero. However, it is found that it is not possible in the numerical time integration approach to find time instant when restoring force vector becomes a null vector. Galerkin's based approach is found suitable for frequency response analysis of

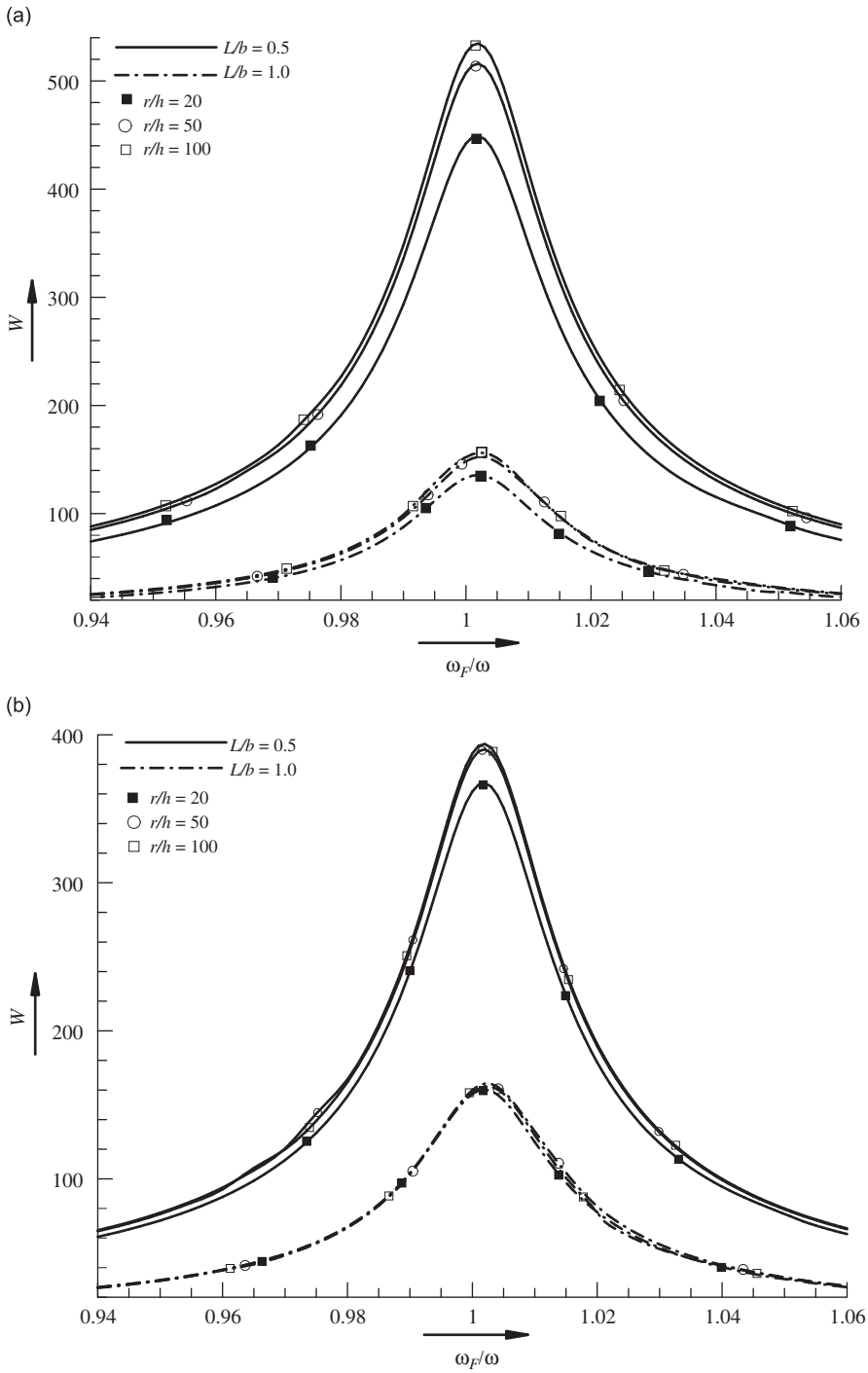

Fig. 14. Frequency response of two-layered cross-ply ($0^\circ/90^\circ$) SSSS panel ($b/h = 10$; $L/b = 0.5, 1$; $r/h = 20, 50, 100$) with in-plane inertia.

bimodular laminated structures. Its application is demonstrated for bimodular cylindrical panels with different geometrical parameters and boundary conditions.

Acknowledgement

Financial support received from Council of Scientific and Industrial Research (CSIR), New Delhi (India) through Grant no. 22(0401)/06/EMR-II is gratefully acknowledged.

References

[1] C.W. Bert, J.N. Reddy, W.C. Chao, V.S. Reddy, Vibration of thick rectangular plates of bimodulus composite material, *ASME Journal of Applied Mechanics* 48 (1981) 371–376.
[2] J.L. Doong, L.W. Chen, Vibration of a bimodulus thick plate, *ASME Journal of Vibration, Acoustics, Stress and Reliability in Design* 107 (1985) 92–97.
[3] J.L. Doong, C.P. Fung, Vibration and buckling of bimodulus laminated plates according to a higher order plate theory, *Journal of Sound and Vibration* 125 (1988) 325–339.
[4] B.P. Patel, S.S. Gupta, R. Sarda, Free flexural vibration behavior of bimodular material angle-ply laminated composite plates, *Journal of Sound and Vibration* 286 (2005) 167–186.
[5] C.W. Bert, M. Kumar, Vibration of cylindrical shells of bimodulus composite material, *Journal of Sound and Vibration* 81 (1982) 107–121.
[6] K. Khan, B.P. Patel, Y. Nath, Free vibration of bimodulus laminated angle-ply cylindrical panels, *Proceedings of the Fourth International Conference on Theoritical, Applied, Computational and Experimental Mechanics ICTACEM* 07, IIT Kharagpur, India, December 27–29, 2007.
[7] K. Khan, B.P. Patel, Y. Nath, Vibration analysis of bimodulus laminated cylindrical panels, *Journal of Sound and Vibration* 321 (2009) 166–183.
[8] K. Khan, B.P. Patel, Y. Nath, Free vibration of bimodulus laminated cross-ply conical panels, *Proceedings of the Ninth Biennial ASME conference on Engineering System Design and Analysis ESDA*08, Haifa, Israel, July 7–9, 2008.
[9] J.N. Reddy, Transient response of laminated, bimodular-material, composite rectangular plates, *Journal of Composite Materials* 16 (1982) 139–152.
[10] B.P. Patel, S.S. Gupta, M. Joshi, M. Ganapathi, Transient response analysis of bimodulus anisotropic laminated composite plates, *Journal of Reinforced Plastics and Composites* 24 (2005) 795–821.
[11] C.W. Bert, Models for fibrous composites with different properties in tension and compression, *Journal of Engineering Materials and Technology, Transactions of ASME* 99H (1977) 344–349.
[12] H. Kraus, *Thin Elastic Shells*, Wiley, New York, 1976.
[13] G. Pratap, B.P. Naganarayana, B.R. Somasekhar, Field consistency analysis of the isoparametric eight-noded plate bending element, *Computers and Structures* 29 (1988) 857–863.
[14] K.J. Bathe, *Finite Element Procedures*, Prentice-Hall, New Jersey, 1996.